DEPLETION ANALYSIS OF THE OPAL REACTOR WITH VESTA

P.Young[1], I. Limaiem[2], E. Ivanov[3], W. Haeck[3]

1) Oakridge Sciences & Services, 8 rue Croix de Malte, 45000 Orléans, France
2) Altran Technologies, 2 rue Paul Dautier, 78140 Vélizy-Villacoublay, France
3) Institut de Radioprotection et de Sûreté Nucléaire (IRSN), BP 14, 92262 Fontenay-aux-Roses Cedex, France

Corresponding author: p.young@oakridge.fr

Abstract. This paper presents and discusses results of static core and depletion analysis of the OPAL research reactor with MCNP and VESTA. Zero power, fresh static core calculations were performed in MCNP with a full 3D model. The model was then evolved with the VESTA burn-up code, the depletion results were verified against experimental data of the reactor status for cycles 007 - 011. The static core calculations were in good agreement with the experimental data; the neutron flux profile calculations revealed a discrepancy which was able to be quantified and explained. The depletion calculation results closely matched the experimental data on the reactor with an absolute positive reactivity bias of 1775 ± 19 pcm at the end of the five cycles.

1. Introduction

VESTA [1] is a code developed by the Institut de Radioprotection et Sureté Nucléaire (IRSN) that couples a Monte Carlo (MC) radiation transport code with an activation/depletion module. It currently works with MCNP [2] or MORET as the transport module and ORIGEN2 or PHOENIX as the depletion module. Transport results (the reaction rates) are automatically passed into the depletion module for nuclide evolution either under decay, constant power or constant flux burn-up.

VESTA's emphasis is on accessibility, (being compatible with previous input files) and performance, VESTA uses a 43,000 binned energy group structure for the tallies to limit calculation time (as compared to a continuous spectrum such as in MONTEBURNS). The coupling is coded generically allowing for great flexibility, so that new predictor algorithms can be included or new advances in the transport package. The code uses a simple header at the beginning of the MC input file. Several interactive features that can be incorporated at the start of each new transport step are essential to this work, they include shuffling of material zones and adjustment of the transformation/translation cards in the MC code. This allows swapping of fuel assemblies, as is done during fuel re-loads and insertion or extraction of the control rods as is done during reactor operation to maintain a critical system.

VESTA is still under development and validation efforts are ongoing for PWR systems. This validation is being extended to research reactors and plate-type fuels for which this work is a first step in that direction.

Open Pool Australia Light water reactor (OPAL) was chosen for study with VESTA since it is modern research reactor and uses plate fuel. Moreover, ANSTO was part of the IAEA Co-ordinated Research Project: Innovative Methods for Research Reactors along with the IRSN. Thus much data was available on the core schematics as well as experimental data acquired during commissioning tests.

OPAL is located in South Sydney, Australia, operated by the Australian Nuclear Science and Technology Organization (ANSTO) and designed by the Argentine company INVAP. It is a

multi-use reactor, providing, neutron beam materials science research and neutron irradiation for radioisotope production, activation analysis studies and commercial semi-conductor doping services. OPAL consists of a small 35 cm x 35 cm core with an active height of 61.5 cm. It is composed of 16 plate type fuel assemblies with ^{235}U enriched to ~19.75 %. The reactor's nominal power is 20 $MW_{thermal}$. The chain reaction is regulated and controlled by four control plates and one control cross (CRs or CRPs) composed of Hafnium. The coolant-moderator is light water, and the core chimney is surrounded by a 1.3 m radius D_2O reflector (which also contains the experimental facilities). This reflector is itself within a light water pool tank of radius 2.25m and 14m in height. The chimney and fuel assembly (FA) cladding is aluminum. The reflector tank is zirc-alloy.

The experimental data against which the computer models will be verified are:

- MCNP Static Model
  - General reactor conditions (criticality, kinetics)
  - CRP differential worth
  - Steady State Thermal Neutron Flux Profiles
- VESTA Evolution Model
  - Reactor depletion for operational cycles 007 - 011

2.1. MCNP Neutronic Model

All features detailed in the neutronic specifications [3] were modeled. This includes the core, core chimney, heavy water reflector, the inner experimental facilities within it and its vessel and vessel jacket, the lower plenum and part of the reactor pool/well. The cadmium wires are 30.8 cm in length with a radius of 0.025 cm. Further refinements and clarifications to the model were done via exchanges with George Braoudakis from ANSTO (particularly for the fuel meat and the exact axial details of the assembly cladding and CRPs). The CRPs and their frame plate, end caps and followers were modeled as best they could be for the data provided. Further information on the modeling can be found in [4].

For the flux profile calculations, the gold wire and their aluminum plates were added to the model. These were modeled as described in [5]. The thermal flux profile ($E < 0.625$ eV) was then calculated along the gold wire in the water channels with an fmesh tally. The tally encapsulates the gold and a tiny bit of water at each ANSTO data point, off the ANSTO points the tally is within the water channel

This model uses ENDF/B-VII.1 cross-section libraries with S(α,ß) and is computed with MCNP6.1. The notational model from the neutronic database [6] is used for the cold neutron source. Sensitivity analysis showed it to be a better representation.
Thermal conditions (density and cross-sections): The cold neutron source is at ambient, standby conditions. The fuel, reflector and moderator are at cold zero power conditions.

2.2. VESTA Specific Modeling & Parameters

The following materials were burned: the fuel meat, the cadmium burnable poison and the hafnium CRPs. Preliminary studies were carried out to determine the optimal number of axial layers for the fuel meat, this was determined to be 40 (see [4]). The fuel composition is differentiated into separate material zones for each of the 16 (active) assemblies, not between separate plates of an assembly. The Burnable Poison (BP) is divided into 5 axial layers, the

material zones is again distinct for each assembly and not for each wire. The CRPs were each divided into 5 axial layers.
Thermal conditions (density and cross-sections): The cold neutron source is at cold, operational status. The reflector and moderator are at full power conditions. The fuel is at cold zero power conditions.

Preliminary sensitivity calculations were carried out on cycle 007 to determine optimal computation conditions. First predictor-corrector was tested simultaneously with a mid-transport step between two critical states. These results yielded negligible differences in the evolution of the core reactivity. Therefore a simple predictor treatment with only a transport step computation at each CRP displacement was retained. A second perturbation was performed with the meat uniformly increased to 63°C via MAKXSF [7] re-processing of the cross-sections. This temperature perturbation had an average impact of -88 pcm at each transport step for the first half of cycle 007 no trend in the difference was observed, so the meat was left at 293.6 K. Finally cycle 007 was computed with a radial zoning of the BP (4 equal volume layers), this produced no impact on the depletion results.

ENDF/B-VII.1 cross-section libraries at 293.6K with S(α,ß) were used for transport and depletion. These are built into VESTA. The exception being for zircon that is burnt in the CRPs, these use ENDF/B-VII cross-sections as VII.1 were not available for depletion in the current VESTA libraries. The internal VESTA depletion module, PHOENIX, was used with the Origen2.2 PWRU50.lib. VESTA 2.1.5 is used. The operation data is in the reactor experiments document [5]: the step and burn history, the CRP positions, the FA load management and the D_2O purity. In the model the heavy water was adjusted at the beginning of each cycle to match the ANSTO measured cycle average D_2O purity. Throughout the cycles investigated, the D_2O was leaking which necessitates this. Cycle 007 is considered a fresh core with zero poisoning as only low powered commissioning test cycles had been previously conducted. The operational data gives the average reactor power output over a specified time period, with the instantaneous CRP positions at the beginning and end of each period. In the VESTA depletion model, the MC transport steps are at each one of these instantaneous positions with the CRP positions adjusted for each MC calculation. The burn period between these two uses the given average power. This will be discussed further later as the blend of instantaneous CRP positions and averaged power complicates the analysis and will provide insight into interpretations of the depletion results.

3.1 Static Core Calculations Primary Results

Table I below presents the calculated results for configuration #1, (the first listed critical state of the control rod worth measurements [5]) along with the average of all the control rod worth measurement critical states and available ANSTO data for comparison. NB: In this paper, all MCNP uncertainties (σ) are at 1 STD.

TABLE I: Primary Results

	k_{eff}	σ	EALF [MeV]	ν_f	β_{eff} [pcm]	σ [pcm]	α_{rossi} [μsec^{-1}]	σ [μsec^{-1}]
Config1	1.00340	0.00008	7.81E-08	2.44	735	9	-4.14E-05	0.06E-05
Avg of critical states	1.00384	0.00008	7.83E-08	2.44	725	9	-4.43 E-05	0.06E-05
ANSTO Data	1 (critical state)	-	-	-	768 (calculated [8])	-	-3.81E-05 (measured by Feynman-α method [9])[1]	-

[1] It was learned later that this measurement was done with 15 rather than 16 FA. This would most certainly be the source of the difference. That 15 FA were used is not reported in the reference document [9].

Below (*FIG.1.*) is the calculated over-reactivity for all of the critical states.

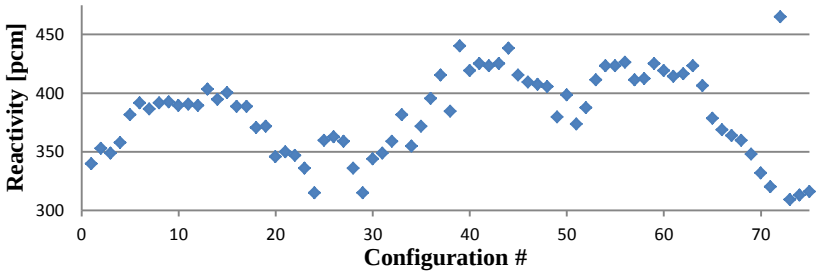

FIG. 1. Critical Configurations

Config#72 had a relatively high k_{eff}, its corresponding differential measurement also produced a differential worth of -4066 pcm. Thus, this data was omitted from the following calculation of the differential worths. The -4066 pcm was likely from the CRP being moved into its next position for the final step measurements, and was not itself a differential measurement.

3.2 Differential Control Rod Plate Worths Results

Below in *FIG. 2.-6.* are the differential CRP worths calculated with the states from the experiments document [5]. As two measurements are made per step movement of a rod, the average of the two calculated worths is used. The errors bars are the MCNP uncertainty. The CRP position is the mid-point of a step insertion. The location of the CRPs in the core is shown in *FIG. 24.* of section 4.5. ANSTO data was provided in $, this was converted to pcm using the ANSTO (INVAP) calculated β_{eff}=768 pcm.

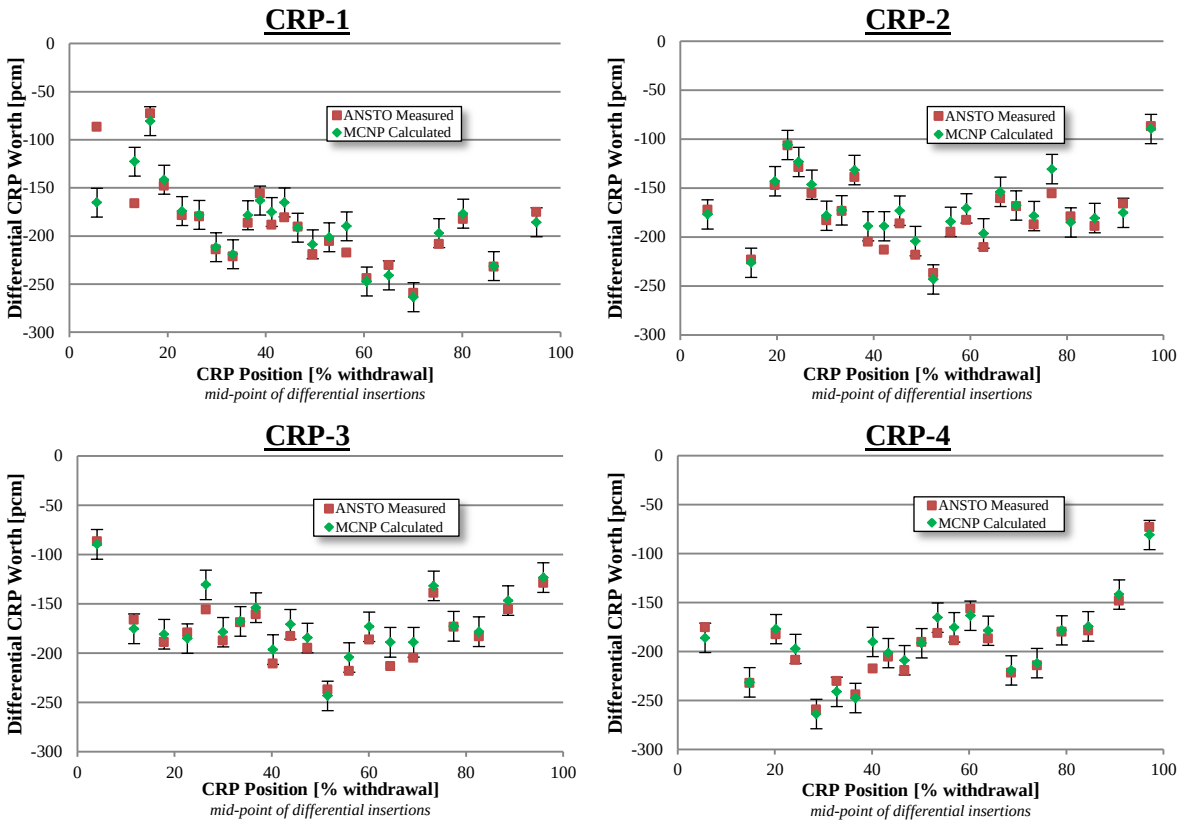

FIGs. 2.- 5. CRP Differential Worths

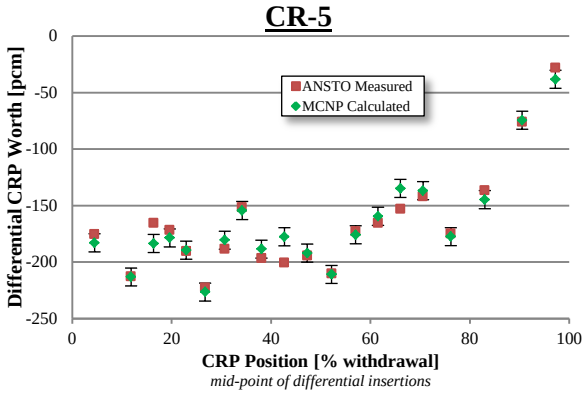

FIG. 6. CRP Differential Worths

These results could be further improved by reducing the standard deviation on the MCNP calculation, but these are intensive long calculations. The experimental data on the positions of the CRPs might also not be as precise as could be desired.

Below in TABLE II is the CRP integral worth, computed by summing the differential worths.

TABLE II: CRP integral worth [pcm]

CRP	ANSTO Measured	MCNP Calculated	Combined MCNP Uncertainty
1	4347	4313	345
2	4375	4221	375
3	3725	3568	315
4	4093	4024	315
5	3329	3321	300

3.3 Thermal Neutron Flux Profiles Results

The MCNP tallies, ϕ_{F4}, were normalized using the following equation as elaborated in [10]:

$$\Phi[\frac{n}{cm^2 s}] = \frac{P \cdot \upsilon_f}{1.6022 \cdot 10^{-13} \cdot w_f \cdot k_{eff}} \cdot \phi_{F4}$$

Where P is the reactor power, ν_f is the average number of neutrons produced per fission, w_f is the average energy deposited in the system by a fission event. ANSTO calculated (based off measurements) the power to be 36 kW +/- 6 kW [5]. ANSTO recommends a value of 201.97 MeV for w_f but [10] recommends 198 MeV. ν_f and k_{eff} are calculated by MCNP. For the scaling factor, three combinations of these variables were verified: a best estimate (BE) with values recommended by ANSTO, a minimal estimate and a maximal estimate.

TABLE III: Tally scaling parameters

	P [kW]	**υ_f**	**w_f** [MeV]	**k_{eff}** (σ= 0.00004)	**e** [J/MeV]
BE	36	2.44	201.97	1.00642	1.6022E-13
Max	42	2.44	198	1.00642	1.6022E-13
Min	30	2.44	201.97	1.00642	1.6022E-13

The determinant factor is the power. The *Max estimate* was the best fit, as seen below in *FIG. 7.-12.* In effect, in [11] they too use a power of 42 kW for scaling. More data is needed on ANSTO's method for determining the reactor power. It seems there is systematic uncertainty, as the flux profiles are close relative matches, but absolutely are only a match at 42 kW. The

error bars on the graph are the MCNP tally uncertainty. The location of the wires in the assemblies is marked in blue on *FIG. 8.*

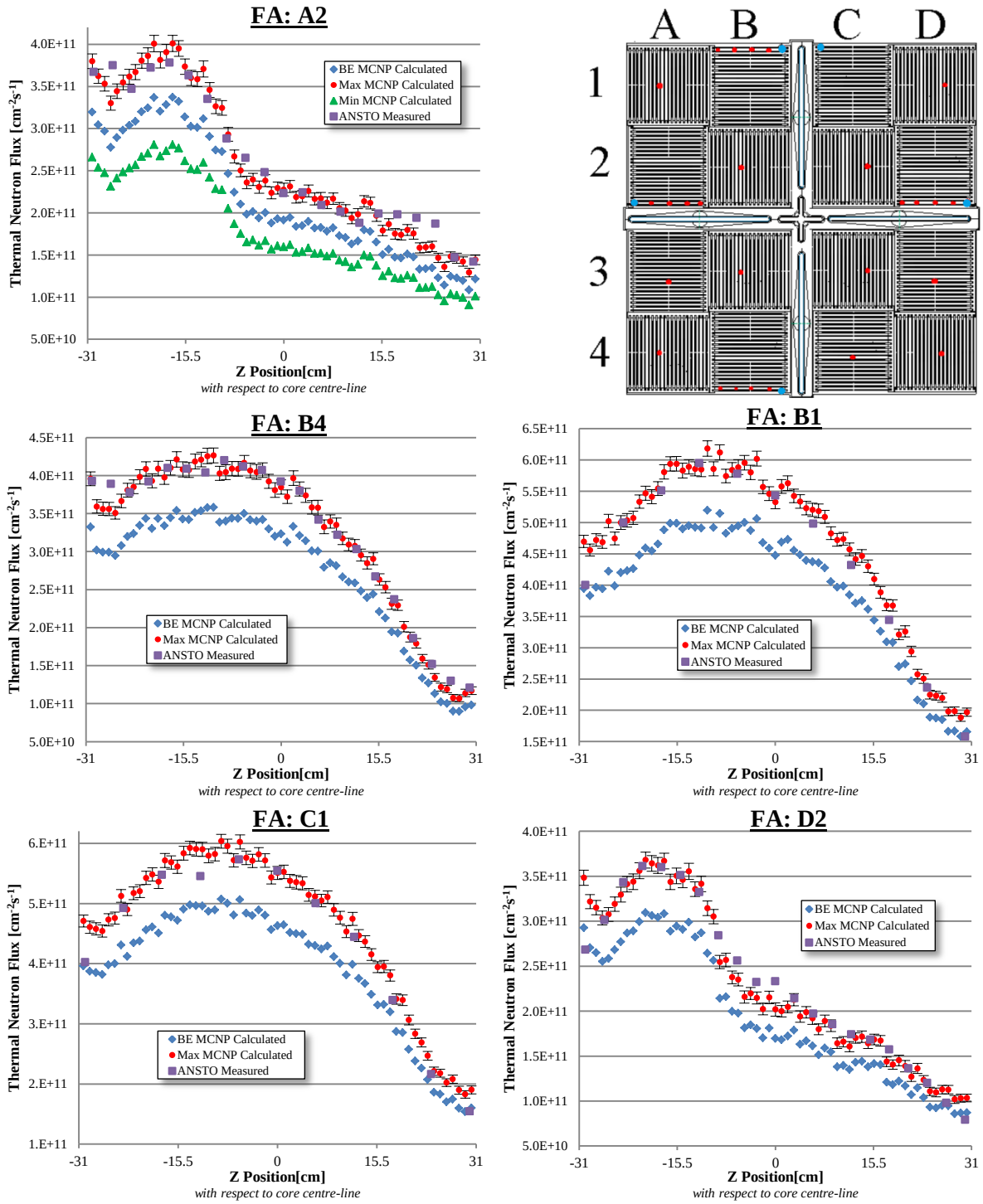

FIGs. 7. - 12. Thermal Neutron Flux Profiles and core locations (core image from [5])

The k_{eff} in the gold wire calculations was 300-400 pcm higher than the previous critical states, the probable reason being that the cadmium covers were not modelled; sensitivity simulations inferred that they have a worth of ~300 pcm. The deviations at the axial ends of the profiles could be due the model incorporating insufficient CRP details (end caps, holding plates, etc.). Looking at D2 between -7 and +5 cm it appears that the control rods have moved and are slightly extracted from the core, since the model flux is relatively depressed there.

3.2 VESTA Depletion Calculation Results

The k_{eff} depletion results for cycles 007- 011 are presented below in *FIGs. 13.-17.*

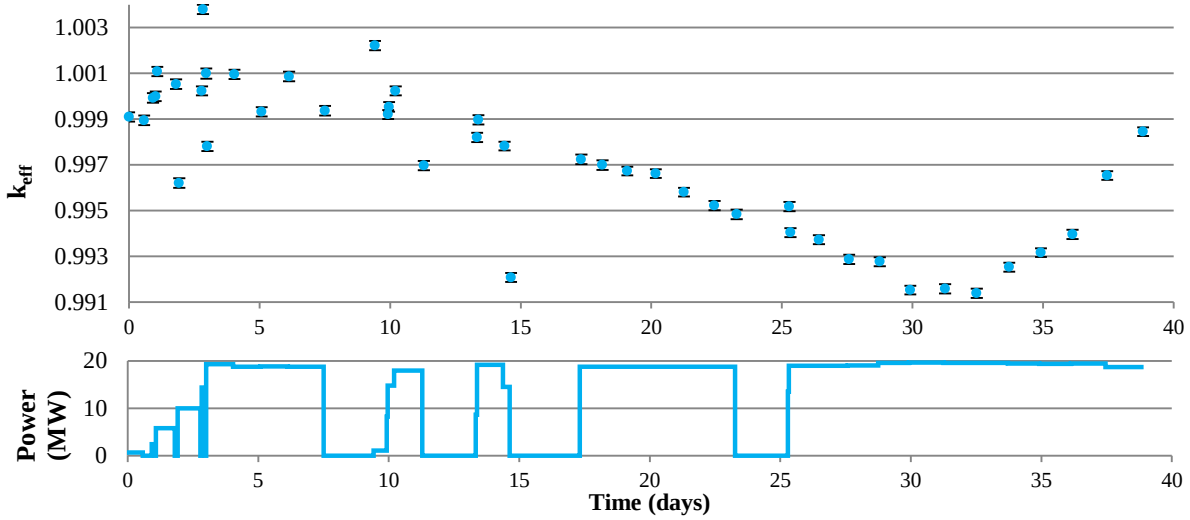

FIG. 13. Cycle 007 Depletion & Power History

It is interpreted that any point that is on the k_{eff} 'trend line' is a reactor critical state. It is interesting to analyze the points that have significantly deviated from the k_{eff} trend by observing their corresponding power history. The deviations off the k_{eff} trend appear to be due to non-critical states and reactor transients. Looking at the points t=11.29 and t=14.63 days in cycle 007 (*FIG.13.*), in the next time step the power immediately goes to zero and the k_{eff} significantly deviates from the trend; the CRP positions are that of a shutdown state.

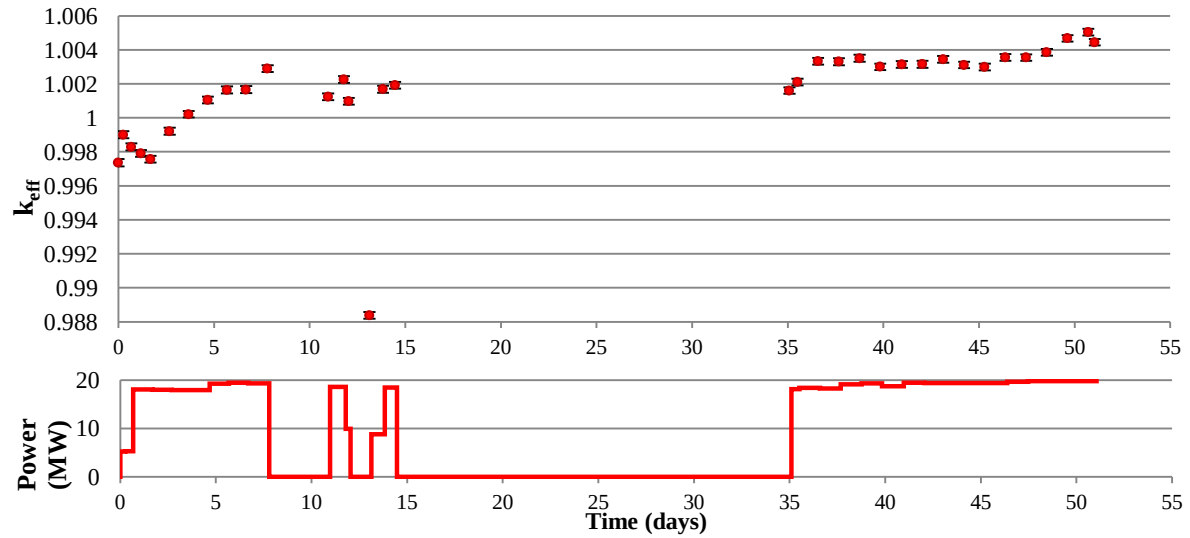

FIG. 14. Cycle 008 Depletion & Power History

At t=12.05 in cycle 008 (*FIG. 14.*) the operating data states that CRP-5 is dropped causing a transient and the reactor was left shutdown for just over a day. Here it seems that the CRP at 12.05 is indeed a critical state but the position at t=13.03 is a shutdown with an under reactivity of ~1300 pcm with respect to the critical state trend line. It would be so negative so to compensate for any Xenon dynamics during the 1 day shutdown. It is a strong confirmation of the code and model that when the reactor returns to power, the critical trend line continues from where it was before the transient.

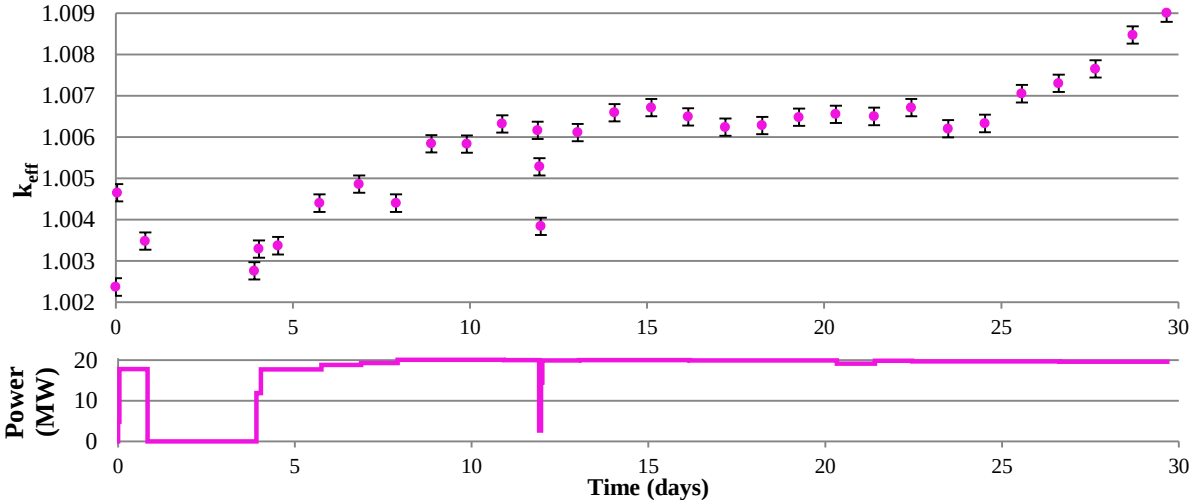

FIG. 15. Cycle 009 Depletion & Power History

In cycle 009 (*FIG. 15.*) at t=11.96 and t=12 days we see another offset from the trend again when a quick 2h transient occurs; a ramp down from 20 MW to 3 MW then back up to 14 MW. It could be that these are non-critical states, or more probably the model is having a hard time following the power/poison transients due to the quick power ramps with little details on the intermediates steps. It could also be other un-modeled system/thermal feedbacks.

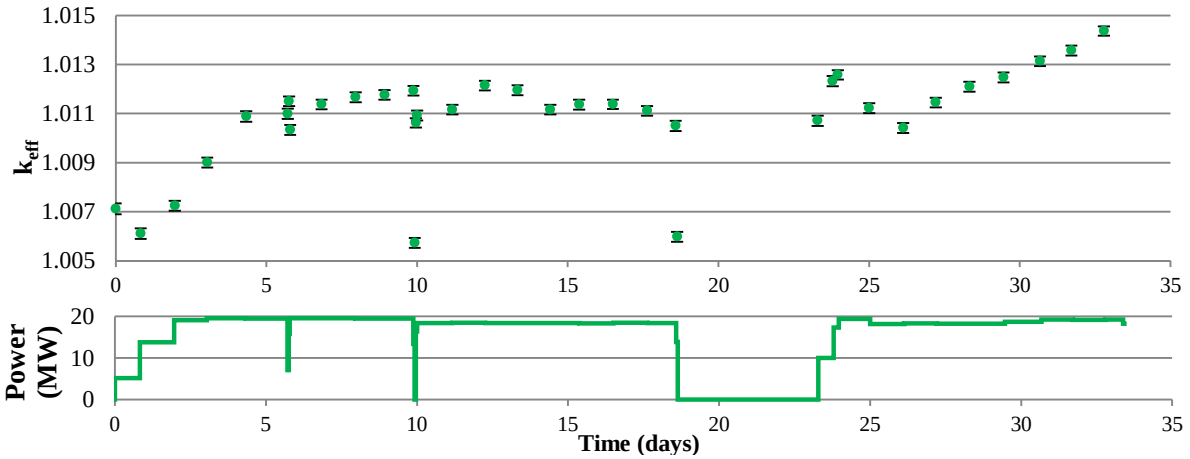

FIG. 16. Cycle 010 Power History

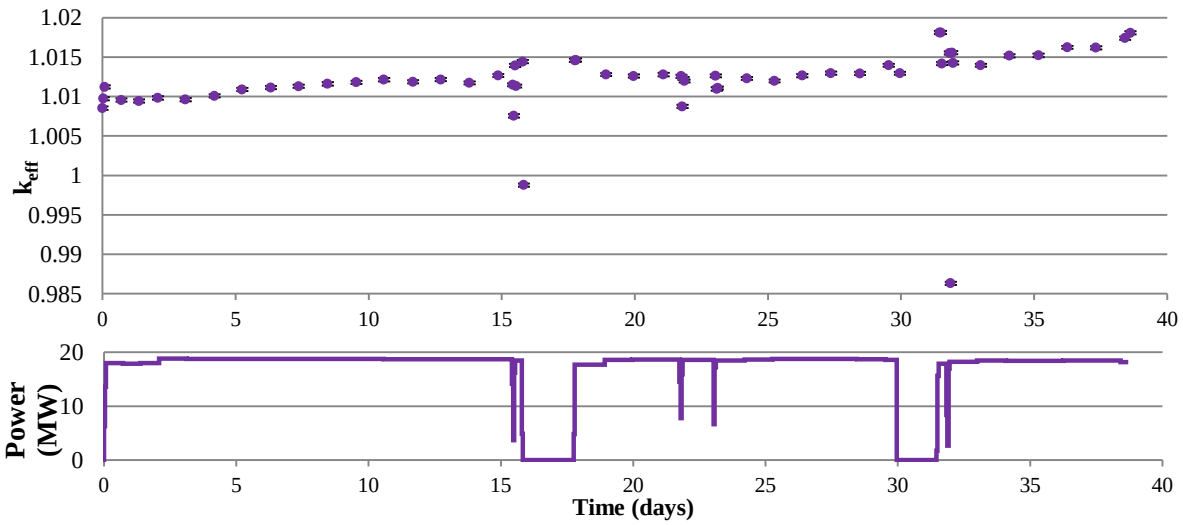

FIG. 17. Cycle 011 Power History

For reference purposes the average D_2O is given below in Table IV.

TABLE IV: Average D_2O purity measured during operating cycles, from [5]

Cycle	D_2O purity[w/w %]
007	97.5
008	97.1
009	96.9
010	99.55
011	99.24
012	98.93

4. Depletion Analysis and Discussion

4.1 All Rods Out Full Power Depletion

A cycle 007 depletion (*FIG. 18.*) was done but with the CRPs withdrawn from the core (All Rods Out (ARO)) and burned at a full 20 MW for 26 Equivalent Full Power Days (EFPD) with MC steps at each EFPD. After the depletion, each MC step was re-computed with the critical CR positions; positions from the operation data that was closest to each EFPD.

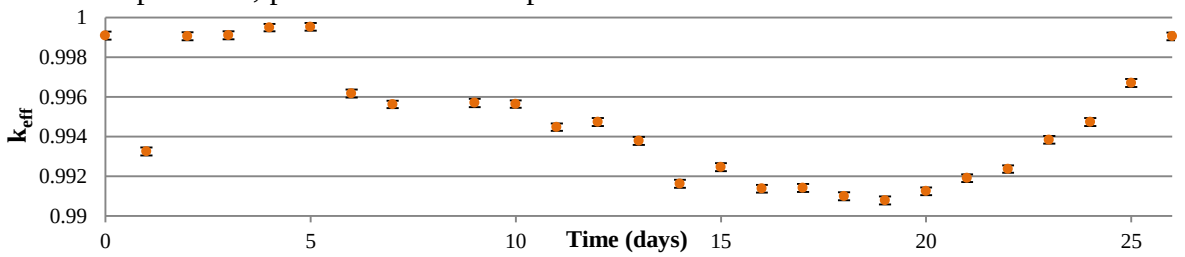

FIG. 18. ARO/EFPD Cycle 007 Depletion with MC steps re-computed after at critical CRP

The k_{eff} trend closely matches that of the critical CRP burn, and at the end of cycle 007 there is only a difference of 60 pcm between the two. An ARO/EFPD depletion seems to produce data that is sufficiently accurate. Inspired by [13].

4.2 k_{eff} Trend

It is interesting to graph together the k_{eff} evolution for all of the cycles (below *FIG. 19.*).

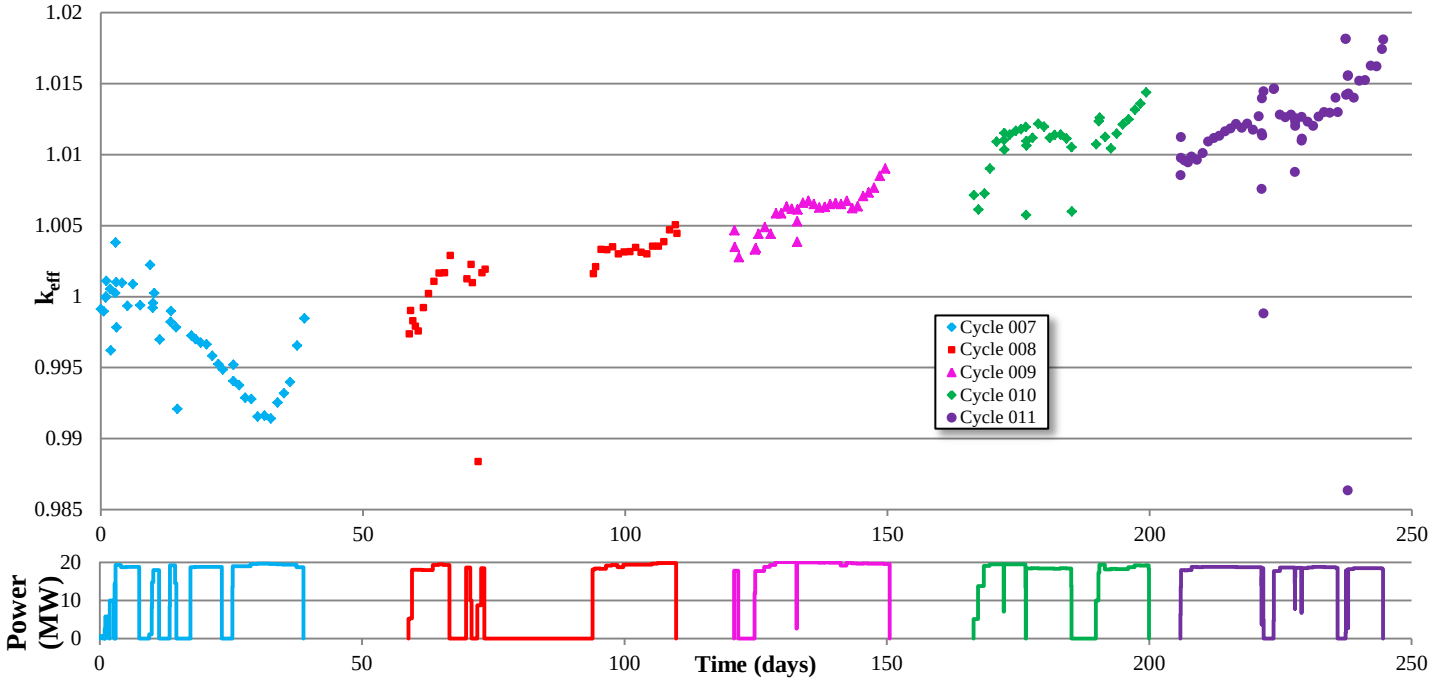

FIG. 19. All Cycles VESTA Depletion

Since the reflector is modeled at a constant average cycle value it is expected that critical states on the trend-line would start (absolutely) under-reactive at the beginning of a cycle and gradually become over-reactive by the end of a cycle. Overall the model reactivity is gradually trending upward over the span of the calculation; there is a common trend between cycles 008-011. When jumping between cycles and adjusting the D_2O, the reactivity doesn't drop as much as could be expected to compensate the increased reactivity produced in the previous cycle. It is unknown why the reactivity steadily drops in cycle 007 from t=10 to t=31 days, perhaps un-modeled feedback effects of the fresh reactor settling to a steady state. Analysis of the results and data is complicated by the operating data's limited details, for instance the measurement time of the CRP could be slightly off which impacts the critical state timing. Also, in the model power ramps suddenly, physically this would be gradual.

Quantitatively, at the end of the five depletion computations the critical state is 1775 ±19 pcm absolutely over-reactive, and 1866 ± 39 pcm over-reactive relative to the initial calculation in cycle 007. More analysis is required, particularly of the transients and pertinent VESTA data.

4.3 Core Isotopic Composition

With the data produced from the VESTA depletion calculation, many aspects of the core can be analyzed and quantified. This is aided in particular by the AURORA [12] depletion analysis tool that is included with VESTA. A sampling is provided here and in 4.3 and 4.4. Below are two graphs that show the evolution of select neutron poisons and pre-cursors in the entire core for cycle 007 (*FIG. 20.*) and 008[2] (*FIG. 21.*).

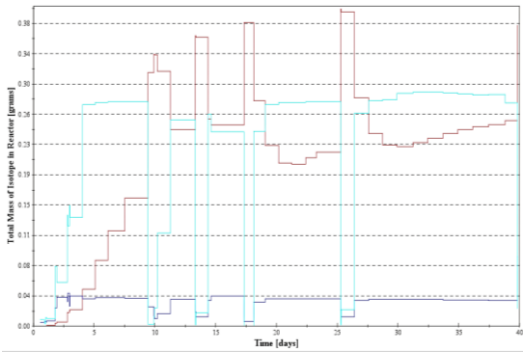

FIG. 20. Cycle 007 select poisons

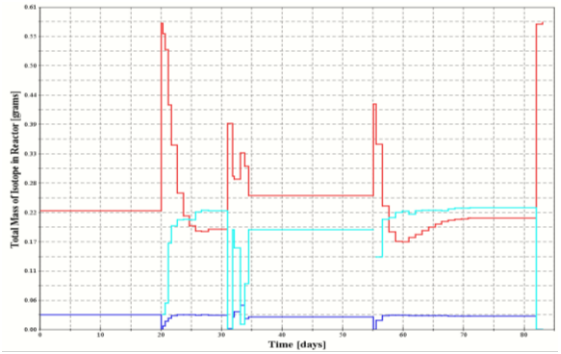

FIG. 21. Cycle 008 select poisons

These step-wise graphs can be misleading and difficult to interpret, as the compositions jumps and then remains constant. The data in fact represents the nuclide composition results at each transport computation. Physically during a shutdown the Sm^{149} would gradually build up rather than a sudden spike, the graphs would be more instructive with mid-point calculations. During the cycle 008 Xenon transient at t=12.05 (t=32.05 here) the Xe^{135} build-up is visible along with other poison dynamics even with such few power steps.

4.4 Decay Heat

VESTA can analyze the isotopic decay heat. This allows determination of the spent fuel assemblies' decay heat after they have been removed from the core and put into storage which is shown in *FIG. 22.* where the decay heat for the assemblies ejected at the end of cycle 007 is shown for their lifetime in the core and for 80 days of decay afterwards.

[2] Cycle 008 here includes at the start the shutdown period of 20 days between cycles 007 and 008.

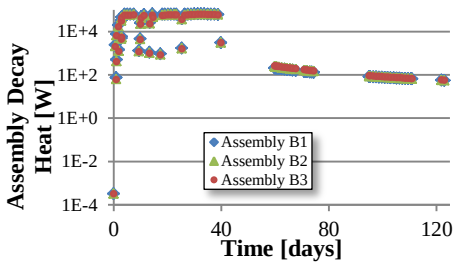

FIG. 22. Fuel assembly decay heat

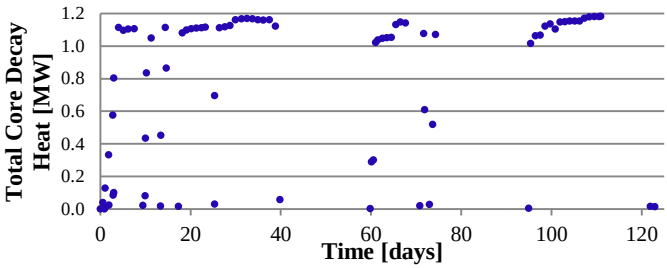

FIG. 23. Core decay heat cycles 007-008

FIG. 23. (above) shows total in-core decay heat for cycle 007 and 008. The reactor decay heat eventually reaches a steady state, at t=31.3 days into cycle 007 the decay heat is 1.17 MW of the full 19.6 MW power output. This equates to 5.97 % of the total power.

4.5 Core Power Distribution

The depletion calculation allows quantification of the power of the different fissile zones. Below (*FIG. 24.*) are several power/BU maps near the start and ends of cycles 007 and 008.

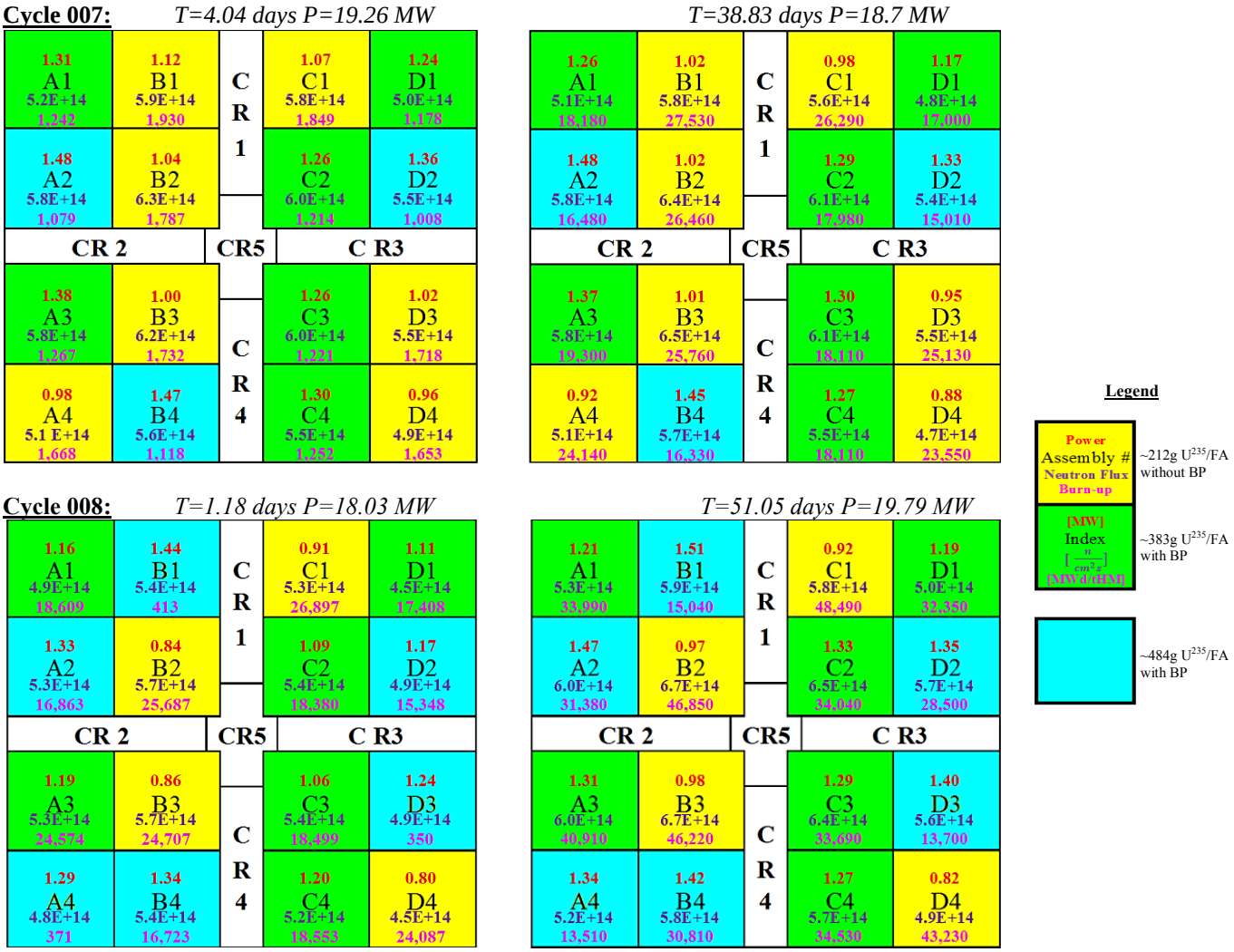

FIG. 24.Core power/flux/BU maps, original figures without BU data from [3]

These maps show that the fuel assemblies with the highest burn-up are those that are removed from the core at the end of cycles 007 and 008. Respectively, B1, B2, B3 and B2, B3, C1.

5. Conclusions

Although the static calculation model largely agreed with the experimental data, the axial flux distribution calculations demonstrated a discrepancy between the BE calculation results and the ANSTO measured scalar flux. Taking into account that the measured and computed relative flux profiles were similar this discrepancy can be explained by the uncertainty in the determination of the reactor power which was 36 ± 6 kW, but for the data to match more closely (in absolute) was likely closer to the 42 kW upper bound. This could be for a number of reasons, shielding effects or time delays in the activation and counting of the gold wires. Since MCNP is a code that is widely used and well validated against many experimental benchmarks it is very likely that the measured values should be re-evaluated in order to provide credible benchmark data. More generally, the instrumentation should also be improved for research reactors and further data provided on the simplifications for power evaluation for better benchmarking. The VESTA model had good results closely matching the experimental data on the reactor evolution for cycles 007 - 011, albeit with a gradually increasing positive reactivity bias. The model produced allows analysis of many additional parameters of the reactor depletion.

6. References

[1] HAECK, W., "VESTA User's Manual - Version 2.1.0", IRSN Report DSU/SEC/T/ 2012-081 Index A, Institut de Radioprotection et de Sureté Nucléaire, France (2012)

[2] GOORLEY, T., et al., "INITIAL MCNP6 RELEASE OVERVIEW - MCNP6 VERSION 1.0", LA-UR-13-22934, Los Alamos National Laboratory, USA (2013)

[3] ANSTO, OPAL Reactor Specification, IAEA CRP 1496: Innovative Methods for Research Reactors

[4] YOUNG, P., Calculs de répartition de puissance et d'évolution effectués à l'aide d'un code Monte Carlo pour des cœurs de réacteurs expérimentaux, M.Eng. Thesis, Institut National des Sciences et Techniques Nucléaires, CEA Cadarache (2011)

[5] ANSTO, OPAL Reactor – Experimental Data", IAEA CRP 1496: Innovative Methods for Research Reactors

[6] INVAP & ANSTO, DATABASE FOR OPAL CALCULATION, IAEA CRP 1496: Innovative Methods for Research Reactors

[7] BROWN, F., "The makxsf Code with Doppler Broadening", LA-UR-06-7002, Los Alamos National Laboratory, USA (2006)

[8] Private correspondence with George Braoudakis

[9] ANSTO, Reactor Physics Measurements on the OPAL Reactor during Commissioning, IAEA CRP 1496: Innovative Methods for Research Reactors

[10] SNOJ, L., "Calculation of Power Density with MCNP in TRIGA reactor", International Conference Nuclear Energy for New Europe 2006, Portoroz, Slovenia, www.djs.si/port2006/

[11] INTERNATIONAL ATOMIC ENERGY AGENCY, Meeting Report of the 4th Research Coordination Meeting of the CRP1496, IAEA CRP 1496: Innovative Methods for Research Reactors, Vienna (2012) (working material)

[12] HAECK, W., "AURORA User's Manual - Version 1.0.0", IRSN Report PSN-EXP/SNC/ 2013-24 Index A, Institut de Radioprotection et de Sureté Nucléaire, France (2013)

[13] FERRARO, D., et al., "OPAL Reactor Full 3-D Calculations using the MonteCarlo Code Serpent 2", IGORR 2014, Bariloche, Argentina , ww.cab.cnea.gov.ar/igorr2014/